Evaluation of a covariance-based clock and ephemeris error bounding algorithm for SBAS

Juan Blanch, Todd Walter, Per Enge.

Stanford University

Abe Stern, Eric Altshuler

Sequoia Research Corporation

ABSTRACT

The largest source of error uncertainty in current Space-based Augmentation Systems, which are single frequency (L1), is the ionospheric delay. In the coming years, the deployment of new signals in L5 will allow civil users to estimate and remove the ionospheric delay in the pseudoranges. This will have a large impact on the planned dual frequency Satellite Based Augmentation Systems (SBAS). Once the ionospheric delay error uncertainty is removed, the Protection Levels will decrease substantially, and other error sources will dominate. The remaining terms in the error bound are much less critical than the ionospheric delay error bound in the current single system, so it is likely that they can still be optimized. This is true in particular for the User Differential Range Error (UDRE) and Message Type 28 (MT28) algorithms which compute the clock and ephemeris error bounds. In [1], we outlined the main elements of a covariance based joint UDRE and MT28, which took into account both biases and receiver faults. Simulations showed that it could reduce VPLs by 20%, potentially enabling more demanding operations like Cat. II approaches. The improvements did not depend on a change in the message standards. In [2], we showed that this algorithm could even bring benefits to the current single frequency Wide Area Augmentation System WAAS, by making coverage less sensitive to the loss of a single satellite, and by strengthening coverage on the coasts of the U.S.

In this work, we further develop and evaluate with WAAS prototype data the algorithm that was presented in [1]. In the first section, we will describe the basic elements of the algorithm, in particular how to overcome the fact that the matrix defined in Message Type 28 is only sent every 120 s, (when the time to alarm is 6 s). In the second part, we will set the tunable parameters of the algorithm and the algorithm using WAAS prototype data. This data is taken from a WAAS prototype that matches the current WAAS operational system. We will evaluate the performance of the algorithm using L1 and L2 pseudorange data and compare it to the current UDRE and MT28 algorithm to determine whether its implementation SBAS would be worthwhile.

INTRODUCTION

As users become increasingly reliant on the Wide Area Augmentation System (WAAS), it will be necessary to maintain or even increase its level of service. In particular, WAAS should be robust to changes in the GPS constellation. Although it is not possible to make WAAS insensitive to any change in the constellation, it might be possible to increase its robustness, especially at the edge of coverage (like the West Coast and Alaska). Although the largest contribution to the error bound comes from the ionospheric delay error bound, it is possible to reduce the protection levels by reducing only the clock and ephemeris error bound [1], [2]. In this paper, we evaluate an evolution of the algorithm presented in [1] using WAAS prototype data. First, we will start by providing the basic elements of a covariance based UDRE and MT28 algorithm, then we will show which parameters need to be tuned and a preliminary tuning, and we will present availability

simulations that use the results of this tuning and compare them to the legacy algorithm.

UDRE AND MESSAGE TYPE 28

For each satellite, the SBAS receiver forms the standard deviation σ_{flt} [3] corresponding to the clock and ephemeris error from two different elements in the broadcast message, the UDRE index and the 4 by 4 upper triangular matrix R included in Message Type 28 [4]. The UDRE index provides the value of σ_{UDRE} and R gives the value of the scaling matrix M ($M = R^T R$). The formula for σ_{flt} is given by:

$$\sigma_{flt}^2 = \sigma_{UDRE}^2 u_{LOS}^T M u_{LOS} \tag{1}$$

The UDRE index is updated at least every 6 s, whereas the matrix M is updated only every 120 s (and has to be valid for 240 s).

ALGORITHM ELEMENTS

The term σ_{flt} must be such that we have with a probability more than one minus the integrity allocation, *PHMI* [1]:

$$\begin{aligned} &\left| u_{LOS}^T \left(x_{Broadcast} - x \right) \right| \leq \\ &K_{MOPS} \sigma_{flt} = K_{MOPS} \sigma_{UDRE} \sqrt{u_{LOS}^T M u_{LOS}} \end{aligned} \tag{2}$$

In Equation (2), u_{LOS} is the line of sight to the satellite whose range is being bounded, $x_{Broadcast}$ is the four element vector of the satellite clock and position after applying the Long Term Corrections and the Fast Corrections [3], x is the actual clock and position, K_{MOPS} is the constant that multiplies the standard deviation of the SBAS position solution standard deviation (and is equal to 5.33 [3]). We note $x_{Estimated}$ the estimated clock and position of the satellite [1]. This estimate is calculated by the WAAS master station from the measurements collected at the WAAS reference receivers, but cannot be transmitted to the SBAS receiver. If the measurements appear to be consistent (for example using a chi-square test), the $x_{Estimated}$ is computed using a standard minimum mean squared estimator with a loose prior on the satellite position. We note *Cov* the overbounding covariance of the estimation error $x_{Estimated}$ [1]. We have, (with probability 1-*PHMI*):

$$\left| u_{LOS}^T \left(x_{Estimated} - x \right) \right| \leq K_{HMI} \sqrt{u_{LOS}^T Covu_{LOS}}$$

$$K_{HMI} = Q^{-1}\left(1 - \frac{PHMI}{2}\right) \tag{3}$$

(The integrity allocation given to the fault of one satellite is PHMI = $4.5\ 10^{-10}$.)

In the actual algorithm, there are additional terms ([1]). Here we omit them to focus on the basic elements. Since $x_{Broadcast}$ is only fully updated every 120 s, it is not possible to provide the best ground monitor estimate $x_{Estimated}$ to the user within the time to alert. To overcome this limitation, we use the triangular inequality to write that:

$$\begin{aligned} &\left| u_{LOS}^T \left(x_{Broadcast} - x \right) \right| \leq \\ &\left| u_{LOS}^T \left(x_{Broadcast} - x_{Estimated} \right) \right| + \left| u_{LOS}^T \left(x_{Estimated} - x \right) \right| \end{aligned} \tag{4}$$

To meet the integrity requirement, it is sufficient to have:

$$\begin{aligned} &\left| u_{LOS}^T \left(x_{Broadcast} - x_{Estimated} \right) \right| + K_{HMI} \sqrt{u_{LOS}^T Covu_{LOS}} \\ &\leq K_{MOPS} \sigma_{UDRE} \sqrt{u_{LOS}^T M u_{LOS}} \end{aligned} \tag{5}$$

To lighten the notations, we will also omit the fact that for each satellite there are as many estimated position solutions are there are stations, because the WAAS threat model must protect against a worse case error measurement at any of the reference stations [1].

Due to additional integrity requirements, we must have as well [1]:

$$\sigma_{UDRE,FLOOR} \leq \sigma_{UDRE} \sqrt{u_{LOS}^T M u_{LOS}} \tag{6}$$

The standard deviation $\sigma_{UDRE,FLOOR}$ is a lower limit on the value of σ_{flt}.

UDRE COMPUTATION

In this section we assume that the MT28 matrix M is fixed, and we show how to compute the UDRE index. From Equation (5), one can see that it is sufficient to have:

$$\max_{u_{LOS}} \frac{\left| u_{LOS}^T \left(x_{Broadcast} - x_{Estimated} \right) \right|}{K_{MOPS} \sqrt{u_{LOS}^T M u_{LOS}}} + \max_{u_{LOS}} \frac{K_{HMI} \sqrt{u_{LOS}^T Covu_{LOS}}}{K_{MOPS} \sqrt{u_{LOS}^T M u_{LOS}}} \leq \sigma_{UDRE} \tag{7}$$

Using the Cauchy-Schwarz inequality we have:

$$\left|u_{LOS}^T\left(x_{Broadcast}-x_{Estimated}\right)\right| = \left|u_{LOS}^T M^{\frac{1}{2}} M^{-\frac{1}{2}}\left(x_{Broadcast}-x_{Estimated}\right)\right| \leq \sqrt{u_{LOS}^T M u_{LOS}}\sqrt{\left(x_{Broadcast}-x_{Estimated}\right)^T M^{-1}\left(x_{Broadcast}-x_{Estimated}\right)} \quad (8)$$

Therefore, the first term in Equation (7) is bounded by:

$$\max_{u_{LOS}} \frac{\left|u_{LOS}^T\left(x_{Broadcast}-x_{Estimated}\right)\right|}{\sqrt{u_{LOS}^T M u_{LOS}}} \leq \sqrt{\left(x_{Broadcast}-x_{Estimated}\right)^T M^{-1}\left(x_{Broadcast}-x_{Estimated}\right)} = \left|R^{-T}\left(x_{Broadcast}-x_{Estimated}\right)\right| \quad (9)$$

For the second term, we have:

$$\max_{u_{LOS}} \frac{K_{HMI}\sqrt{u_{LOS}^T Cov u_{LOS}}}{K_{MOPS}\sqrt{u_{LOS}^T M u_{LOS}}} \leq \frac{K_{HMI}}{K_{MOPS}} \max_{|x|=1} \sqrt{x R^{-T} Cov R^{-1} x} \leq \frac{K_{HMI}}{K_{MOPS}}\sqrt{\max\left(eig\left(R^{-T} Cov R^{-1}\right)\right)} \quad (10)$$

The UDRE index, noted UDREI is given by:

$$UDREI = \min\left\{\begin{array}{l} i \mid \dfrac{\left|R^{-T}\left(x_{Broadcast}-x_{Estimated}\right)\right|}{K_{MOPS}} \\ +\dfrac{K_{HMI}}{K_{MOPS}}\sqrt{\max\left(eig\left(R^{-T} Cov R^{-1}\right)\right)} \leq \sigma_{UDRE,i} \\ \&\sigma_{UDRE,FLOOR} \leq \sigma_{UDRE,i} R_{44} \end{array}\right\} \quad (11)$$

The second condition implies the constraint expressed in Equation (6). This can be verified by writing that the vector u is of the form:

$$u = \begin{bmatrix} v & 1 \end{bmatrix}^T \quad (12)$$

We then write:

$$u^T R^T R u = \left|Ru\right|^2 = \left\|\begin{bmatrix} R_{1:3,1:3} & R_{1:3,4} \\ 0 & R_{44} \end{bmatrix}\begin{bmatrix} v \\ 1 \end{bmatrix}\right\|^2 = \left\|\begin{bmatrix} R_{1:3,1:3} & R_{1:3,4} \end{bmatrix} v\right\|^2 + R_{44} \geq R_{44} \quad (13)$$

One can see from Equation (11) that the UDRE index must account for the change in the solution separation and the change in observability due to the change in geometry. This computation is performed by the master station at 1 Hz (although the user only needs a 6 s time to alert).

MESSAGE TYPE 28 COMPUTATION

Equation (11) ensures that the integrity requirement is met for any choice of a positive semi-definite scaling matrix M. In this section, we propose a method to compute M. From Equation (5), we can see that in order to efficiently bound the second term, it is desirable to have M be as similar to Cov as possible (that is, that their ratio is a multiple of the identity). However, as indicated before Cov changes every second, whereas M needs to be valid for 240 s (it is updated every 120 s, but it must remain valid for 240 s).

We start by determining a positive semi-definite matrix A:

$$A = \left(\frac{K_{fa}+K_{HMI}}{K_{MOPS}}\right)^2 Cov_{t=0} \quad (14)$$

The matrix $Cov_{t=0}$ is simply the covariance of $x_{Estimated}$ at the time MT28 is computed. The parameter K_{fa} is tunable, and is meant to be an upper bound of the solution separation term [1]. The next step consists on modifying A so that the minimum value constraint (6) is met. The method provided in [1] uses the singular value decomposition of A. Here we provide a method that only requires a Cholesky decomposition. We note R^0 the upper triangular matrix such that $R^{AT}R^A = A$. One can verify that for any line of sight plus clock vector u_{LOS}, we have:

$$u_{LOS}^T A u_{LOS} \geq \left(R_{4,4}^A\right)^2 \quad (15)$$

We define R_{pn} ("pn" stands for pre-normalization) as:

$$\begin{aligned} R_{pn,ij} &= R^A{}_{ij} \text{ if } i \neq 4 \text{ and } j \neq 4 \\ R_{pn,44} &= \max\left(R^A{}_{44}, \sigma_{UDRE,FLOOR}\right) \end{aligned} \quad (16)$$

The next step consists on normalizing R so that when the UDRE index is computed using Equation (11), the UDRE index is in a region where the discretization is adequate. One way of doing this is to normalize R by $\sigma_{UDRE,i}$ for a certain index. Here we choose to normalize by the $\sigma_{UDRE,i}$ corresponding to i defined as:

$$i_{MT28} = \max\left\{ i \mid \sigma_{UDRE,i} \le R_{pn,44}, \sigma_{UDRE\_floor} \le \sigma_{UDRE,i} \right\} \quad (17)$$

As shown in with Equation (13), $R_{pn,44}$ is an upper bound of the minimum value of the projection of $R_{pn}{}^{T} R_{pn}$ over all lines of sight u.

We define R_{pd} ("pd" standing for pre-discretization) as:

$$R_{pd} = \frac{1}{\sigma_{UDRE,i_{MT28}}} R_{pn} \quad (18)$$

The matrix R_{pd} is then discretized, for example as described in [4], with one difference however: the (4,4) element is rounded to a larger value (this guarantees that the minimum value condition expressed in Equation (17) is preserved after discretization) and . The MT28 matrix R is the result of such discretization.

Additional terms

MT28 and the UDRE must also account for:

- the fact that any one measurement coming from a WAAS reference station could be erroneous
- the nominal biases affecting the reference receivers.

In [1] it is described how to bound these terms (which are not naturally expressed in terms of a covariance) by a multiple of a quadratic form.

PRELIMINARY TUNING

The only parameter that needs to be tuned is the parameter K_{fa}.

Data

24 hours of WAAS prototype data were used for this very preliminary tuning. This data comes from an exact replica of the operational code. For each of the 38 WAAS Reference Stations and each satellite in view, one pseudorange measurement is computed every second from the three receivers present at each reference station as well as a measurement noise standard deviation. This process is similar to the one described in [9]. Then the WAAS corrections (computed by the Corrections Processor [10]) are applied to each of the edited pseudorange measurements. This set of measurements is used to compute $x_{Estimated} - x_{Broadcast}$ and the covariance Cov as described in [1].

UDRE index

In Figure 1 we show the difference between the UDREI index computed when determining MT 28 with Equation (17) and the UDREI index computed every second with Equation (11) when using K_{fa} = 5. One can see that most of the time these two indices are identical, which means that during the lifetime of MT 28, the UDRE index rarely changes. Also, when it changes, it appears to be as likely to be reduced as to be increased. The very few large increases correspond to the rapid degradation in the geometry as the satellite sets.

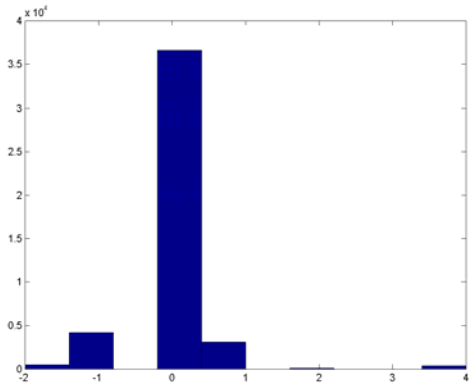

Figure 1. *Difference between the UDRE index determined when computing MT 28 and the actual UDRE index (computed every second)*

In addition, we measured how many times the UDRE index was updated. For the single frequency standard, a rapid updated rate is not an issue. For the dual frequency standard that is being developed, rapid updates in all satellites could be an issue [8]. For two satellite passes of PRN5 (44757 s in total), the UDRE was updated 305 times. This means that it was updated an average of once every 146 s, which is well within the capacity of the dual frequency standard. However, it will need to be determined how these updates are distributed in time. We have shown here the analysis for one satellite; the results were very similar for the other satellites.

AVAILABILITY RESULTS

WAAS performance is estimated using the MATLAB Availability Simulation Tool (MAAST) [7], a service volume model tool that computes the Protection Levels (PLs) that would be experienced by WAAS users. MAAST simulates the WAAS message (GIVE, UDRE, and MT 28, without accounting for events that deviate from nominal behavior), determines the geometries experienced by users, computes the corresponding pseudorange error models, and calculates the PLs.

For the simulations, it was assumed that the UDREI remained constant for the duration of the validity of the MT28 matrix *R* and matched the value computing it (Equation (17)). The covariance UDRE algorithm includes the bias terms that were described in [1], but omitted in the description above.

Single frequency results

PLs were computed for a one by one degree grid of users over North America for a period of 24 h every 300 s. Each map shows the 99% quantile of the VPL at every location as computed by MAAST, configured to simulate current WAAS performance.

For Figure 2 and 3 we used the almanac corresponding to August 28th, 2012, but we removed PRN 21. This satellite was chosen because it actually was out for maintenance between August 28th and August 29th, 2012 [8]. It can be seen that there is a significant loss of coverage of 35 m VPL (necessary for LPV-200), and even 50 m VPL.

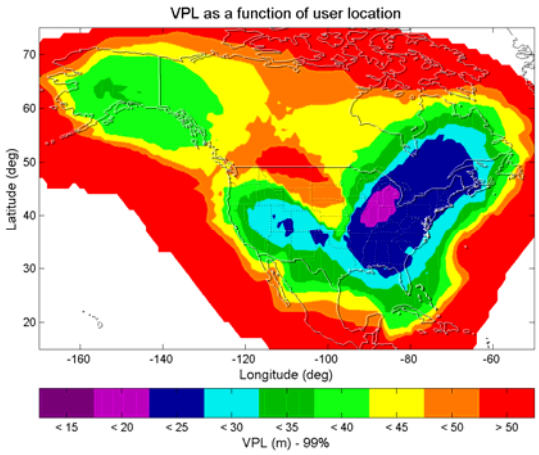

Figure 2. *Map of the 99% VPL quantile with the current UDRE algorithm for single frequency WAAS and PRN 21 out*

In Figure 3, it can be seen that the new algorithm significantly mitigates the effect of the outage: LPV-200 service is regained in most of Alaska and there is no loss of LPV-250 in CONUS. More generally, coverage is improved in all of the edge of coverage.

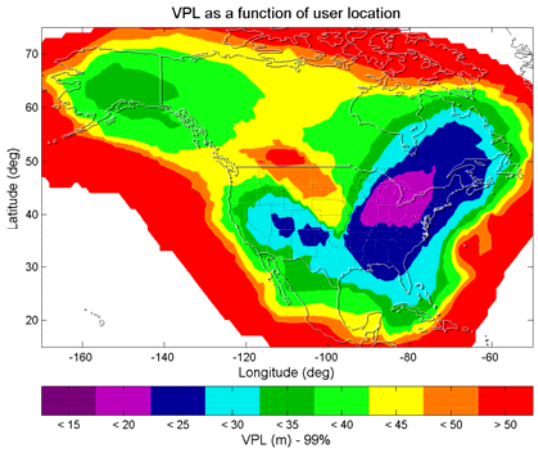

Figure 3. *Map of the 99% VPL quantile with the proposed covariance UDRE algorithm for single frequency WAAS and PRN 21 out*

The results with the baseline 24 satellite GPS constellation are shown in Figures 4(current algorithm) and 5 (proposed algorithm). Again, the proposed covariance UDRE algorithm expands the coverage of LPV-200 at the edge of coverage by a significant amount. In particular, we can see that, with the new algorithm, almost all of the California coast is covered.

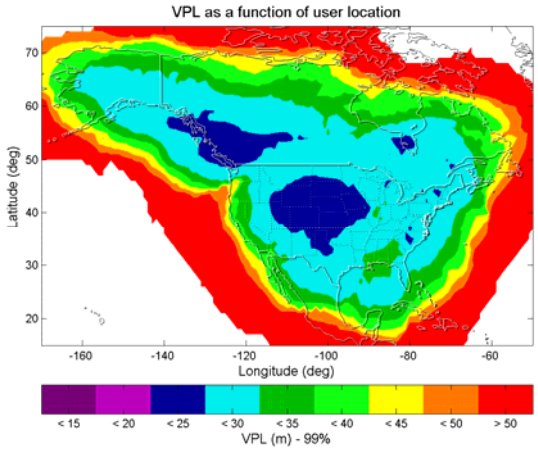

Figure 4. *Map of the 99% VPL quantile with the current UDRE algorithm for single frequency WAAS and the baseline 24 satellite GPS constellation*

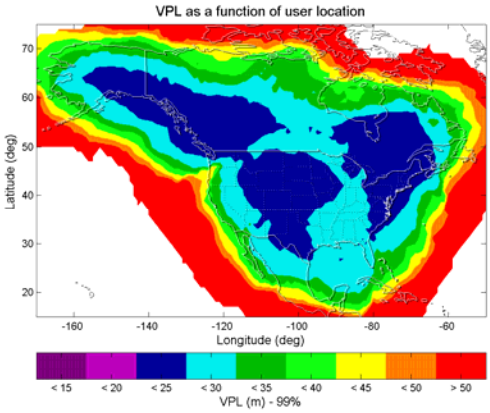

Figure 5. *Map of the 99% VPL quantile with the proposed covariance UDRE algorithm for single frequency WAAS and the baseline 24 satellite GPS constellation*

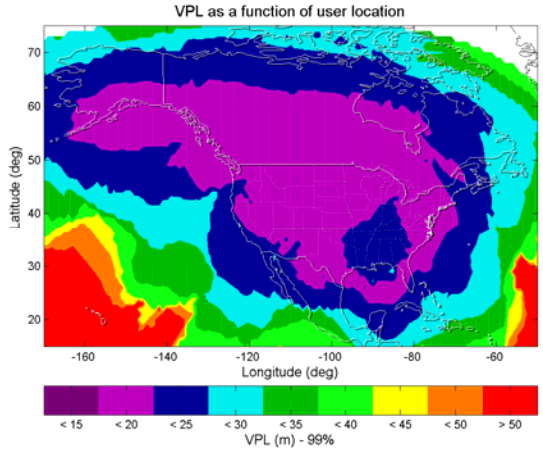

Figure 6. *Map of the 99% VPL quantile with the current UDRE algorithm for dual frequency WAAS and the baseline 24 satellite GPS constellation*

Dual frequency results

For the dual frequency results, the user receiver estimates directly the ionospheric delay using the ionospheric-free combination. The receiver does not use the SBAS computed ionospheric delay estimates and error bounds. However, the uncertainty in the measurement must account for the amplification of the code noise and multipath due to the iono-free combination [8]. Figure 6 shows the performance that would be obtained with the legacy algorithm, and Figure 7 uses the proposed covariance UDRE algorithm. As expected, there is a very significant reduction in the PLs across the service volume. For example, a 20 m VPL is achieved in most of North America. This could potentially enable levels of service more demanding than LPV-200.

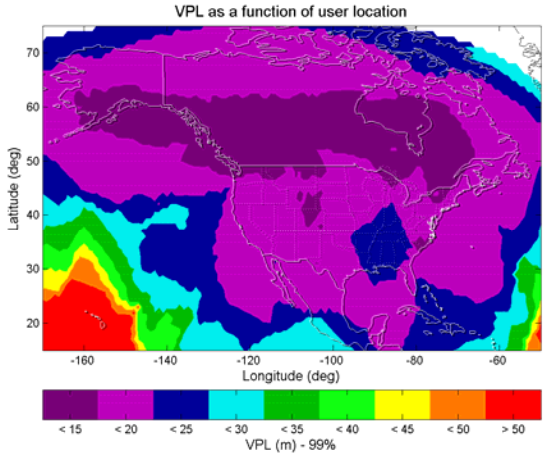

Figure 7. *Map of the 99% VPL quantile with the proposed covariance UDRE algorithm for dual frequency WAAS and the baseline 24 satellite GPS constellation*

SUMMARY

We have described the basic elements of a clock and ephemeris algorithm for SBAS and evaluated its performance in the WAAS case. The constants used by the service volume analysis tool were determined using real prototype data, which ensures that the availability simulations are representative of what the actual performance would be. The simulation results confirm what was already observed in [1] and [2]: the implementation of this algorithm for single frequency WAAS would significantly improve performance at the edge of coverage. Even in the West Coast, where the geometry of the reference stations is problematic, we can observe an expansion of the LPV-200 service area. For a future dual frequency WAAS, in addition to an improvement at the edges, we observe that the VPLs are reduced from 25 m to 20 m in large areas of North America. This would make it easier to consider more demanding levels of service for dual frequency WAAS (and all SBAS systems).

ACKNOWLEDGEMENTS

This work was sponsored by the FAA GPS Satellite Product Team (AND-730).

REFERENCES

[1] Blanch, J., Walter, T., Phelts, R.E., and Enge, P.," Near Term Improvements to WAAS Availability," *Proceedings of the Institute of Navigation International Technical Meeting 2013*, San Diego, January 2013.

[2] Blanch, J., Walter, T., and Enge, P., "A Clock and Ephemeris Algorithm for Dual-Frequency SBAS," *Proceedings of the Institute of Navigation GNSS-11*, Portland, September 2011.

[3] WAAS Minimum Operational Performance Specification (MOPS), RTCA document DO-229D

[4] Walter, Todd, Hansen, Andrew, Enge, Per, "Message Type 28," *Proceedings of the 2001 National Technical Meeting of The Institute of Navigation*, Long Beach, CA, January 2001, pp. 522-532.

[5] Schempp, Timothy R., Peck, Stephen R., Fries, Robert M., "WAAS Algorithm Contribution to Hazardously Misleading Information (HMI)," *Proceedings of the 14th International Technical Meeting of the Satellite Division of The Institute of Navigation (ION GPS 2001)*, Salt Lake City, UT, September 2001, pp. 1831-1837.

[6] Wu, T., Peck, S., "An Analysis of Satellite Integrity Monitoring Improvement for WAAS," *Proceedings of the 15th International Technical Meeting of the Satellite Division of The Institute of Navigation (ION GPS 2002)*, Portland, OR, September 2002, pp. 756-765.

[7] Jan, Shau-Shiun, Chan, Wyant, Walter, Todd, Enge, Per, "Matlab Simulation Toolset for SBAS Availability Analysis," *Proceedings of the 14th International Technical Meeting of the Satellite Division of The Institute of Navigation (ION GPS 2001)*, Salt Lake City, UT, September 2001, pp. 2366-2375.

[8] Walter, T., Blanch, J., Enge, P., "Implementation of the L5 SBAS MOPS," *Proceedings of the 26th International Technical Meeting of The Satellite Division of the Institute of Navigation (ION GNSS 2013)*, Nashville, TN, September 2013, pp. -.

[9] Shallberg, K., Sheng, F., "WAAS Measurement Processing; Current Design and Potential Improvements," *Proceedings of IEEE/ION PLANS 2008*, Monterey, CA, May 2008, pp. 253-262.

[10] Schempp, T., Kung, K."One Decade of WAAS Lessons" November 2008. Available at:

http://scpnt.stanford.edu/pnt/PNT11/2011_presentation_files/15_Kung_et_al-PNT2011.pdf